



## **Introduction to seismic analysis of coupled composite plate shear walls – concrete-filled (CC-PSW/CF)**

Morgan R. Broberg<sup>1</sup>, Soheil Shafaei<sup>2</sup>, Jungil Seo<sup>3</sup>, Amit H. Varma<sup>4</sup>, Shubham Agrawal<sup>5</sup>

### **Abstract**

Understanding the characteristics of the seismic response of coupled composite plate shear walls – concrete-filled (CC-PSW/CF) systems is integral to their use and adoption in practice. Currently, a FEMA P695 study is underway to develop recommendations for the seismic design, response modification factor (R factor), overstrength factor ( $\Omega_0$ ), and deflection amplification factor ( $C_d$ ). The FEMA P695 process involves: (i) designing archetype structures representative of the design space, (ii) developing and calibrating numerical models, and (iii) and subjecting these numerical models to factored ground motions until failure. The study is targeting an R factor of 8 for the CC-PSW/CF system. This paper summarizes the development, modeling, analysis, and results of one such archetype structure. The numerical models for composite walls and coupling beams were developed and calibrated using experimental results. The archetype structure design was modeled using these calibrated numerical models. Nonlinear static pushover and incremental dynamic (nonlinear time history) analyses were performed to characterize the seismic response. The adjusted collapse margin ratio (3.2) for this structure exceeds the lowest limit set in FEMA P695 (2.2). Further analysis of archetype structures representing the entire design space is being performed. Comprehensive results from these analyses will be used to finalize recommendations for the seismic design, response modification factor, overstrength factor, and deflection amplification factor for CC-PSW/CF.

### **1. Introduction**

Core walls are a key part of tall building construction. Conventionally, these elements are coupled reinforced concrete walls, but recently, coupled composite plate shear walls - concrete-filled (CC-PSW/CF) have emerged as a viable alternative. These coupled walls are comprised of composite walls and coupling beams. Composite wall elements consist of steel faceplates with concrete infill. These steel plates are connected with ties bars to ensure composite action. A depiction of a composite plate shear wall – concrete-filled (C-PSW/CF) is included in Fig. 1. Coupling beam members are rectangular steel box sections filled with concrete. These components are prefabricated, shipped to the site, erected, and then filled with concrete. Experimental studies have investigated the lateral wall behavior (Wang et al. 2018) and coupling

---

<sup>1</sup> Graduate Research Assistant, Lyles School of Civil Engineering, Purdue University, <mroberg@purdue.edu>

<sup>2</sup> Graduate Research Assistant, Lyles School of Civil Engineering, Purdue University, <sshafaei@purdue.edu>

<sup>3</sup> Research Engineer, Lyles School of Civil Engineering, Purdue University, <seo2@purdue.edu>

<sup>4</sup> Karl H. Kettelhut Professor in Lyles School of Civil Engineering, Purdue University, <ahvarma@purdue.edu>

<sup>5</sup> Graduate Research Assistant, Lyles School of Civil Engineering, Purdue University, <agraw101@purdue.edu>

beam response (Nie et al. 2014). These studies establish a baseline for creating finite element models to analyze the seismic response of full-scale buildings. Of specific interest is the seismic design factors defined by ASCE 7-16 including  $R$  (response modification factor),  $C_d$  (deflection amplification factor), and  $\Omega_0$  (overstrength factor). A FEMA P695 – Quantification of Building Seismic Performance Factor study is currently under way to offer recommendations for these factors. Archetype structures representative of typical buildings are designed, modelled, and subjected to ground motions as part of this study (FEMA P695). One such archetype structure is detailed and analyzed in this paper.

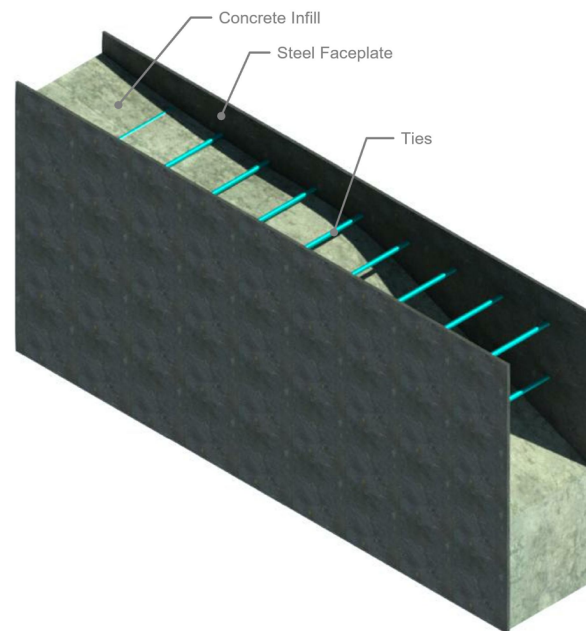


Figure 1: C-PSW/CF cross section

## 2. Archetype Structure

The FEMA P695 procedure requires development of archetype structures representative of the design space. For the CC-PSW/CF system currently being studied, this design space is defined as 8, 12, 18 and 22 story building with coupling beam span to depth ratios of 3, 4, or 5. These structures were designed to withstand earthquake loads representative of Seismic Design Category D regions.

In addition to defining the design space, seismic response coefficient ( $R$  factor) and deflection amplification factor ( $C_d$ ) were selected in order to define seismic loads. An  $R$  factor for CC-PSW/CF is not currently provided in ASCE 7, but the FEMA procedure requires the assumption of an  $R$  factor to initiate design and later analysis to confirm the adequacy of the assumed  $R$  factor. Uncoupled C-PSW/CF systems have an  $R$  factor of 6.5; however, the coupled C-PSW/CF system is expected to have additional system level ductility due to the spread of plastic hinging and inelastic deformations in the coupling beams along the height of the structure. The seismic modification coefficient ( $R$  factor) was assumed to be 8, and the deflection amplification factor ( $C_d$ ) was assumed to be 5.5. An  $R$  factor of 8 is in line with current recommendations for concrete coupled core walls (ASCE 7-16).

This paper summarizes the results of incremental dynamic (nonlinear time history) analyses conducted on an 8-story archetype structure with coupling beam span-to-depth ratio of 4. This structure is designed for  $D_{max}$  seismic loads corresponding to an  $S_{DS}$  of 1.0g and an  $S_{D1}$  of 0.6g

(FEMA P695). This structure is depicted in Fig. 2. Section sizes were selected to meet all relevant strength, deflection, and detailing requirements without significant margin (overstrength). In other words, the structure was designed to be challenged by design basis and maximum considered earthquakes.

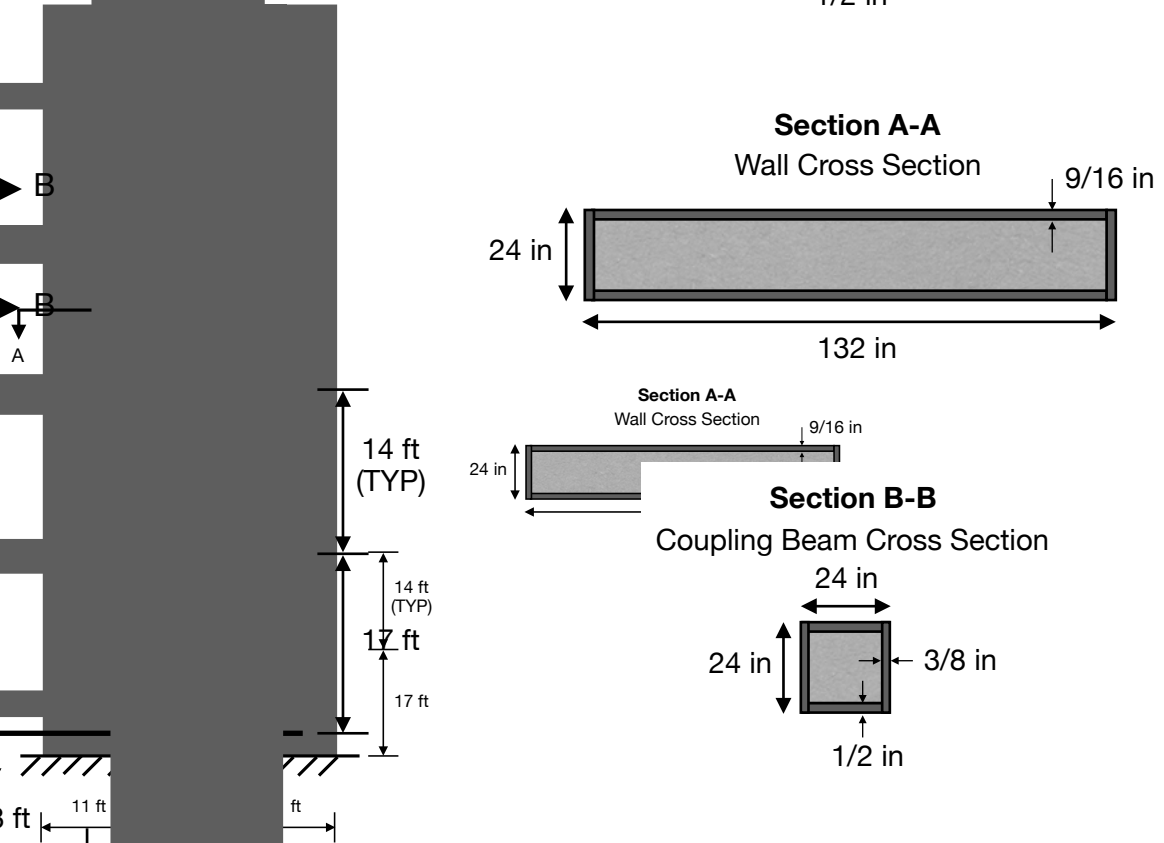


Figure 2: Elevation and cross-sectional geometry of archetype structure

### 3. Model Development

After developing an archetype design, the structure was modelled using OpenSees software (McKenna et al. 2016). The composite wall and coupling beam behaviors were modeled and calibrated separately to corresponding test results. The archetype structure was modeled and analyzed using the calibrated models.

#### 3.1 Composite Wall Behavior

The composite wall behavior was modeled using fiber elements with nonlinear material behavior over the plastic hinge length. The behavior was verified using existing planar wall tests performed at Purdue University (Wang et al. 2018). Material effective stress-strain curves were developed to account for concrete confinement provided by the steel module and compression buckling of the steel plates. These effective stress-strain curves were derived and validated using detailed 3D finite element analysis performed in ABAQUS. The development of these curves is detailed in a companion paper to this text (Shafaei et al. 2019). The concrete stress-strain behavior was defined using the model developed by Tao et al. (2013) with a residual capacity of  $0.6f'_c$ . The steel material model used is elastic-plastic with strain hardening in tension and elastic-plastic in compression. These material models are shown in Fig. 3. Due to the limitations

of the steel material model in OpenSEES, the tension and compression yield stress ( $F_y$ ) could not be asymmetric, which was recommended by Shafaei et al. (2019) based on 3D finite element modeling of behavior. As a result, the steel model in Figure 3 was more conservative (in terms of tensile stress capacity) than recommended. OpenSees wall models were built using these material models. Fig. 4 shows the cyclic lateral load-displacement response for one of the planar wall specimens tested at Purdue (more details are included in Shafaei et al. 2019). The figure includes comparison of the experimentally measured and analytically predicted lateral load-displacement responses. As shown, the OpenSEES model predicts the experimental cyclic behavior reasonably and conservatively (as expected).

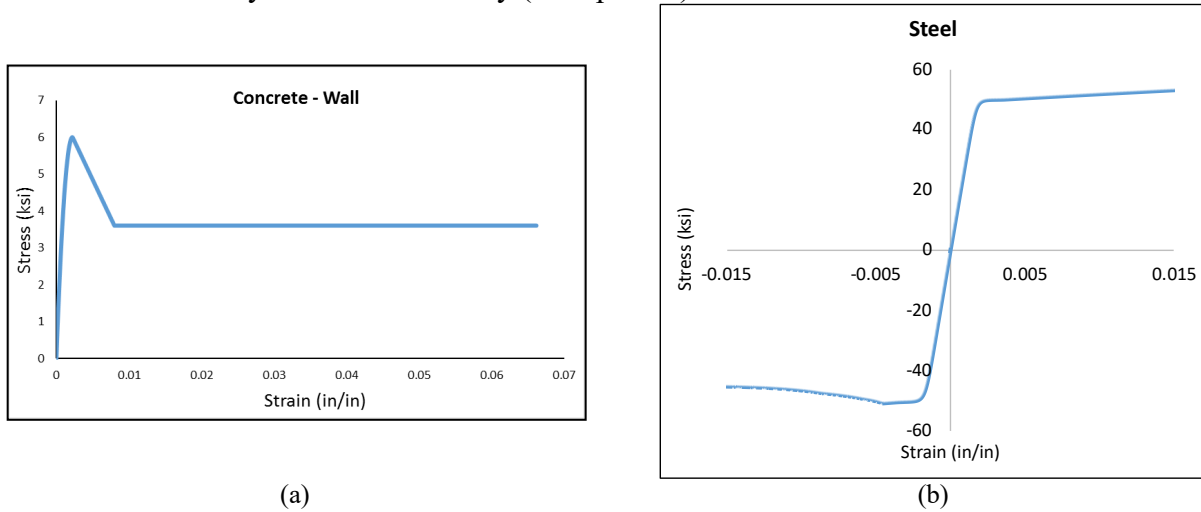


Figure 3: Wall material models for (a) concrete and (b) steel

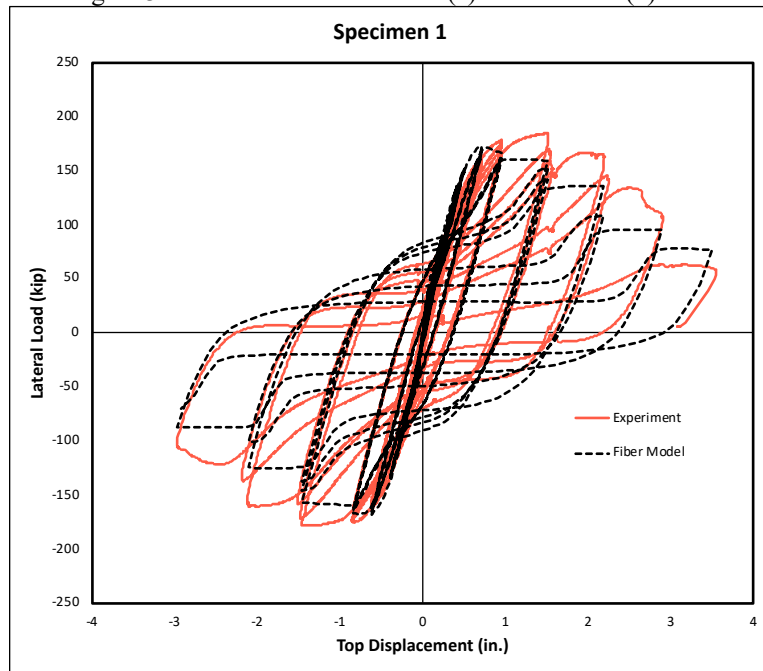


Figure 4: Force versus displacement curves for specimen 1

### 3.2 Coupling Beam Behavior

Archetype coupling beam behavior was modeled using concentrated plasticity elements. These elements model the moment-rotation behavior of the coupling beam plastic hinge without

representing the physical geometry or material behavior but have to be calibrated based on expected behavior. The element was chosen because of its computationally efficiency and ease. Calibrating this non-physical plastic hinge to the geometry and behavior of the designed archetype coupling beam was a two-step process as described in this sub-section. First, a distributed plasticity model was developed to model the nonlinear inelastic behavior of the coupling beam, particularly the plastic hinge regions. This model was verified using the experimental results from coupling beam tests reported in Nie et al. (2014). Then, the verified distributed plasticity element was used to predict the behavior of the archetype coupling beam design, and the results were used to calibrate and define the expected behavior of the concentrated plasticity element.

### 3.2.1 Material Behavior for Distributed Plasticity

Effective stress-strain curves were developed for the steel and concrete fibers of the distributed plasticity element modeling the coupling beam cross-section. The stress-strain curves implicitly accounted for the effects of concrete confinement and steel local buckling. Similar to the wall effective stress-strain curves, these models were developed based on the results of detailed 3D finite element models (analyzed using ABAQUS). The effective stress-strain models are shown in Fig. 5. The concrete behavior follows the model presented by Tao et al. (2013) as modified by Lai et al (2014) with an adjusted the peak stress of  $0.85f'_c$  and plastic post peak behavior for rectangular cross-sections. The steel behavior is elastic-plastic with strain hardening in tension.

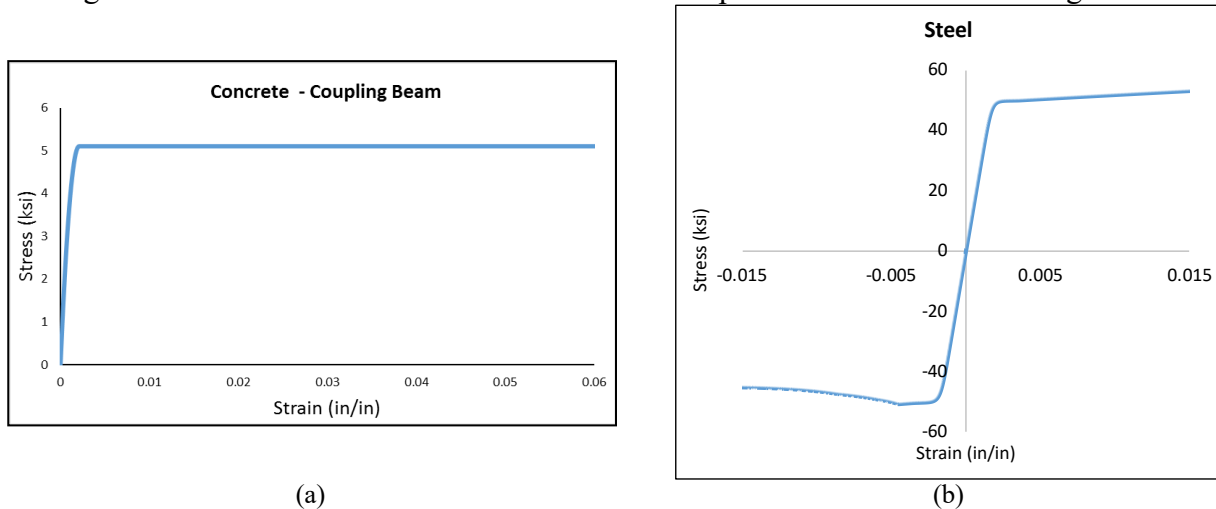


Figure 5: Coupling beam material models for (a) concrete and (b) steel

### 3.2.2 Distributed Plasticity Model

An OpenSees distributed plasticity model was developed for the coupling beams using the material models and element distribution. Over the hinge length (defined as half the depth of the section), four equal length elements were assigned appropriate section geometry and nonlinear material behavior. An elastic element with cracked transformed properties was used in between the two hinges. Displacement-controlled cycles were applied similar to those described in tests by Nie et al. (2014). This model is depicted in Fig. 6(a). As shown in Fig. 7, the force-deformation response predicted using the model followed the measured experimental behavior with reasonable accuracy. Peak forces are calculated accurately, and cyclic degradation matched reasonably; this correlation confirms that the effective stress-strain models were reasonable.

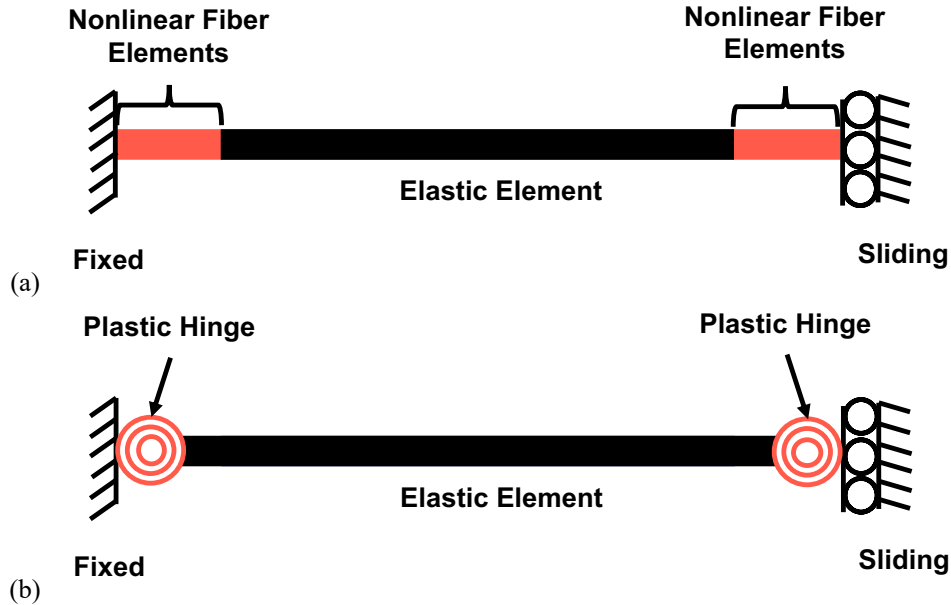


Figure 6: Depiction of coupling beam models (a) distributed plasticity (b) concentrated plasticity

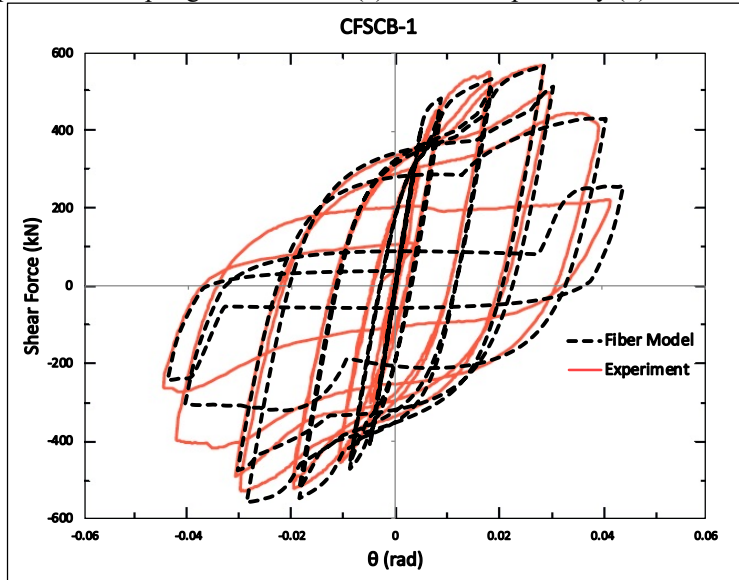


Figure 7: Comparison of OpenSees distributed plasticity model and experimental testing data (Nie et al. 2014).

### 3.2.3 Concentrated Plasticity Model

The coupling beams of the archetypes were first modeled and analyzed using the distributed plasticity model (Fig. 6a) along with the material effective stress-strain curves (Fig. 5). The results from these analyses were then used to calibrate the moment-rotation behavior of the plastic hinges in the concentrated plasticity-based model for the archetype coupling beam, which is shown in Fig. 6b. The results from the distributed plasticity analyses were used to define an envelope curve for moment-rotation behavior of the plastic hinge. This was followed by selecting parameters defining the cyclic behavior including the reloading, deterioration and unloading stiffness. The modified Ibarra-Medina-Krawinkler deterioration model with pinched hysteretic response was used to define the plastic hinge elements (Lignos et al. 2011). Fig. 8 shows the envelope of the moment-rotation behavior for the plastic hinges. The envelope curve is defined by a plastic rotation of 0.025 rad and the ultimate rotation capacity of 0.05 rad. Fig. 9

compares the cyclic moment-rotation behavior predicted by the distributed plasticity and the corresponding concentrated plasticity model for the archetype structure coupling beams. The plastic hinge behavior is modeled conservatively by the concentrated plasticity model, where the yield and ultimate moment capacity are modeled accurately, but the cyclic deterioration and hysteresis are more punitive. This conservative behavior was expected, and also acceptable for the seismic analysis of the archetype structures.

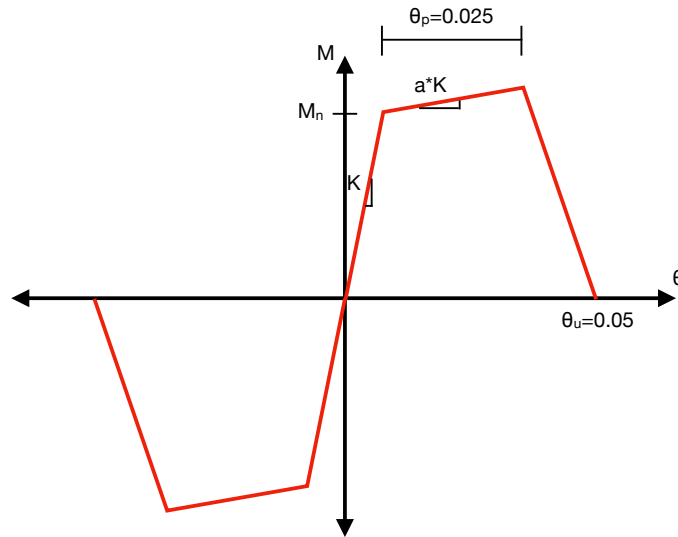


Figure 8: Envelope curve for archetype coupling beam

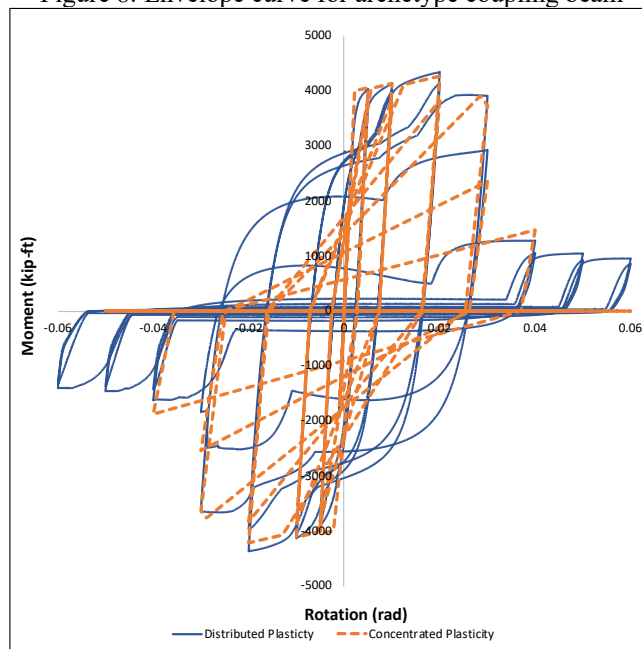


Figure 9: Coupling beam moment-rotation behavior for distributed and concentrated plasticity elements

### 3.2.4 Archetype Structure Model

After developing the composite wall and coupling beam models, the components were combined together to model the whole archetype structure. This model incorporates nonlinear fiber elements at the base of the wall and concentrated plasticity coupling beams. Other important components include the rigid links attaching the coupling beams to the wall elements and elastic

elements used above the nonlinear wall zone and between concentrated plasticity elements. The walls are fixed at both bottom nodes. An overview of the model is presented in Fig. 10. This model also includes a P-Delta column (not pictured). The seismic weight is applied to the P-Delta columns at story height and the column is attached to the walls by rigid links.

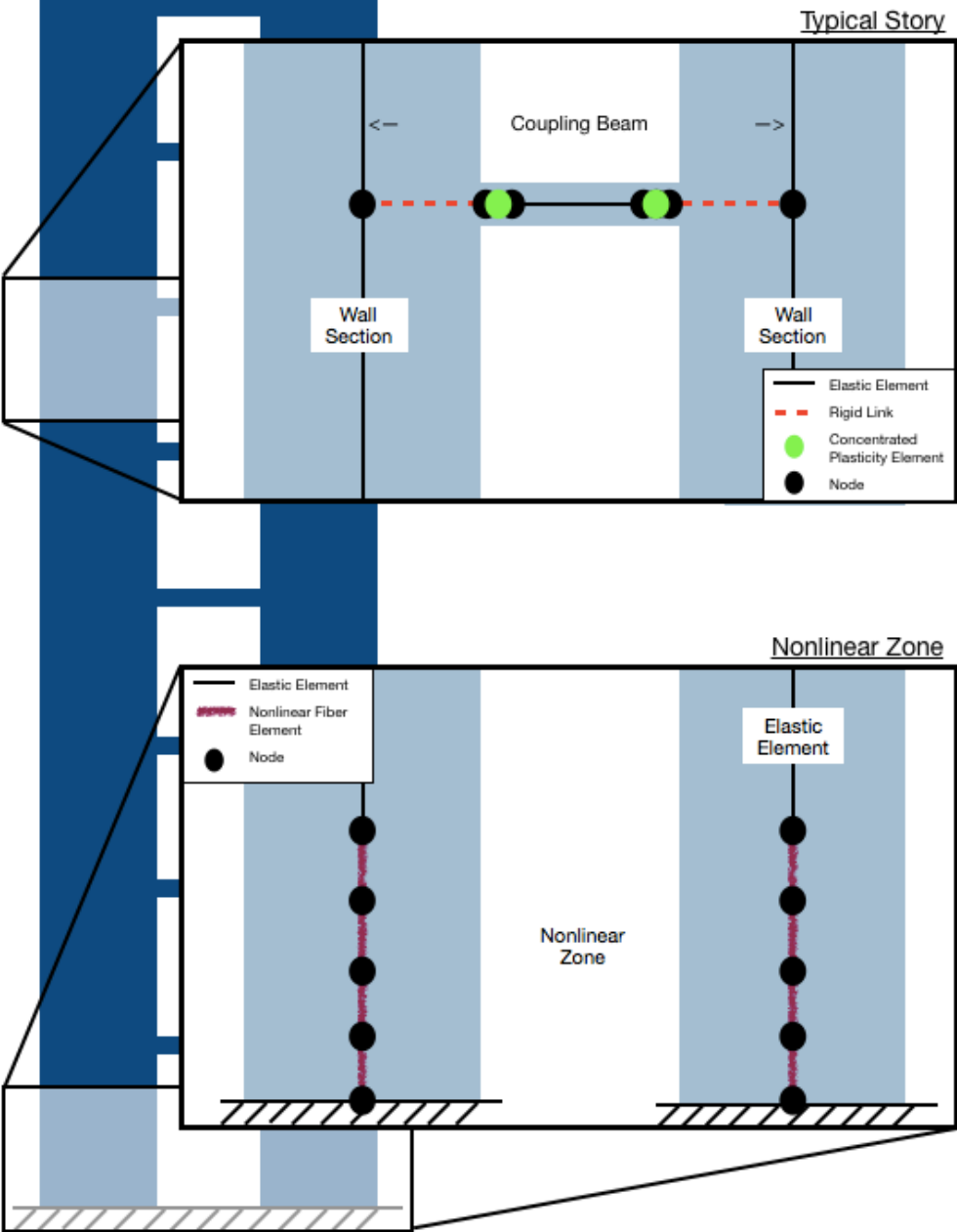


Figure 10: 8-story structure model components

**4. Analysis**

The archetype model was subjected to two types of analysis: nonlinear static pushover and nonlinear time history. The system overstrength factor ( $\Omega_0$ ) and period-based ductility factor ( $\mu_t$ ) can be calculated from the nonlinear static pushover behavior. Nonlinear time history analyses of

the structure are performed for 44 selected ground motions scaled until the structure fails, in line with the FEMA P695 incremental dynamic analysis procedure. These results are then used to determine the spectral acceleration of earthquake corresponding to the median collapse and collapse margin ratio (CMR), the ratio of the median failure earthquake spectral acceleration to the maximum considered earthquake spectral acceleration.

#### 4.1 Pushover Behavior

Pushover loads proportional to the first mode shape were applied to the structure. The pushover curve is plotted in Fig. 11. Point A represents the formation of the first plastic hinge in a coupling beam. The analysis then progresses to Point B. This loading corresponds to formation of plastic hinges in all the coupling beams. The overstrength factor ( $\Omega_0$ ) as defined by the FEMA P695 procedure is calculated from this curve. The overstrength factor for this structure is 2.1.

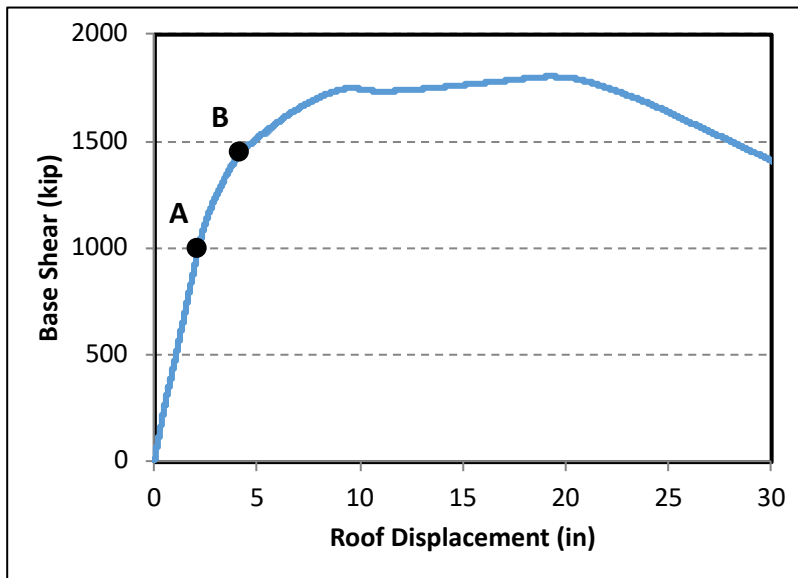


Figure 11: Base shear versus roof drift plot for archetype structure

#### 4.2 Time History Response

The model was also subjected to acceleration time history records. These records represented 22 different earthquakes (2 perpendicular components per earthquake, total of 44 ground motions) and were normalized as specified by FEMA P695. The ground motion records were then scaled up until the structure failed. Complete failure can be difficult to model using fiber-based models that are mostly flexure behavior dominated, and non-simulated failure modes can occur at extremely large interstory drifts (>5%) leading to overall collapse. Therefore, an interstory drift ratio (IDR) of 5% was also used to define failure.

Plots showing the roof displacement versus time for a Superstition Hills (record SUPER ST/B-ICC090) ground motion with increasing scale factor are shown in Fig. 12. The structural response can also be processed to determine the maximum interstory drift ratios. Plots can then be developed for spectral acceleration as a function of IDR. The IDR for the Superstition Hills record is shown in Fig. 13. This plot shows a nearly linear relationship between maximum interstory drift ratio and spectral acceleration in the region of interest.

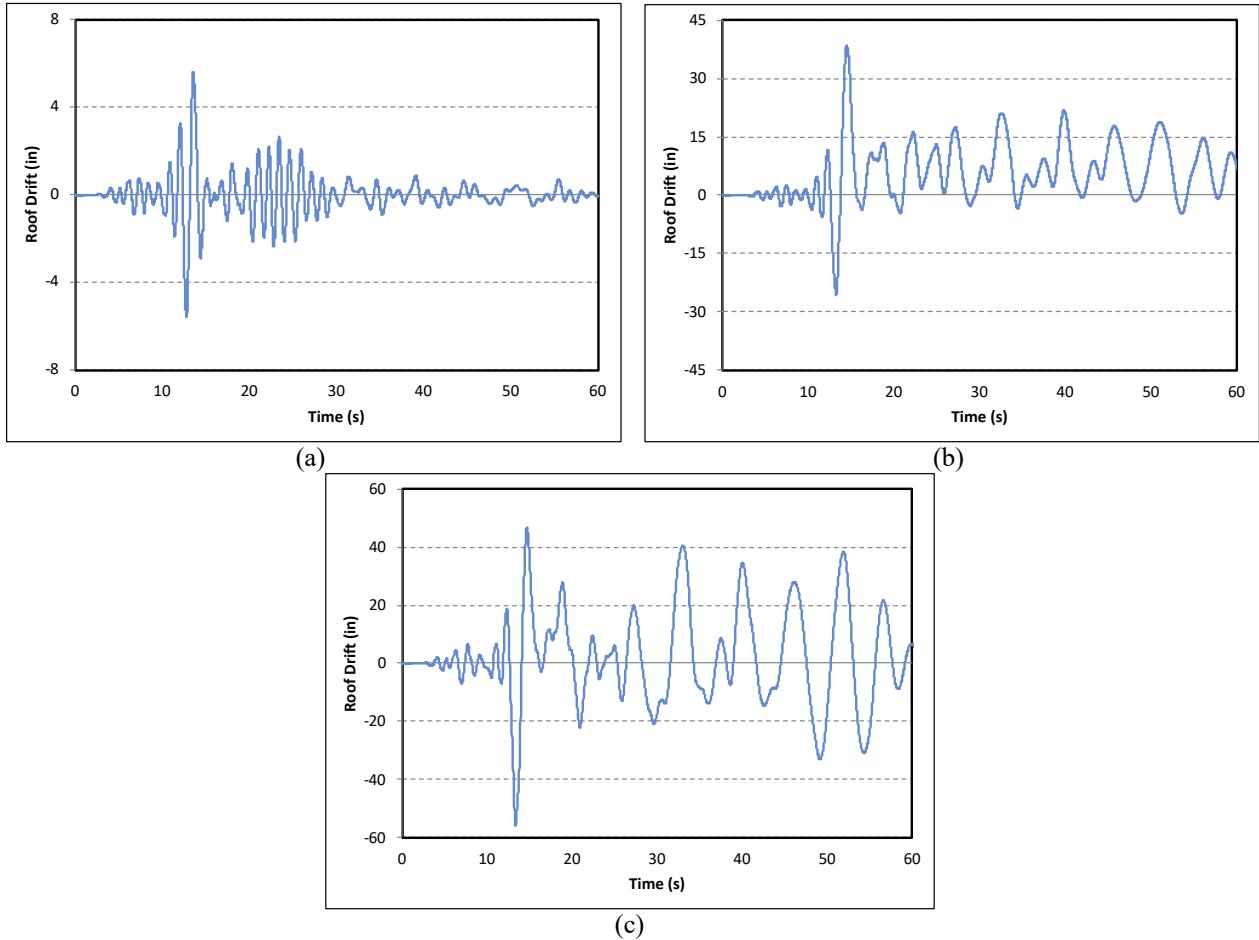


Figure 12: Roof drift versus time for increase intensity for a normalized Superstition Hills ground motion (SUPER ST/B-ICC090) at scale factors of (a) 1, (b) 3, and (c) 6

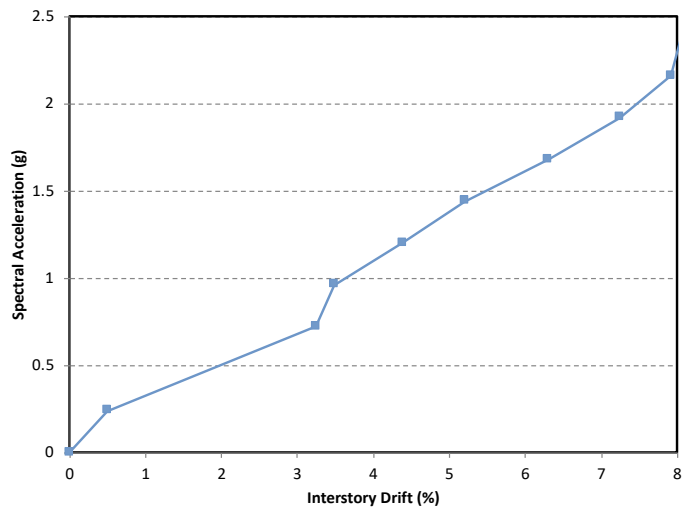


Figure 13: Incremental Dynamic Analysis curve for Superstition Hills (SUPER ST/B-ICC090)  
 Fig. 14 shows the primary results, i.e., the max. story drift ratio vs. spectral acceleration, from incremental dynamic (time-history) analyses conducted for the ground motions. This plot shows that the structure is not equally challenged by all ground motions but that the linear trend observed in the Superstition Hills IDR plot is mirrored in other results. The median failure

spectral acceleration is 2.11g. The collapse margin ratio is 2.5. This value represents the median failure spectral acceleration normalized by the maximum considered earthquake spectral acceleration. The adjusted collapse margin ratio (ACMR) is 3.2. This value accounts for the structure’s period and period-based ductility factor. This value must be evaluated in the context of the remainder of the archetype structure results to confirm a system R factor, but alone the archetype passes the lowest FEMA P695 ACMR threshold value of 2.2 (if all  $\beta$  factors are given a ‘poor’ rating). This structure passes with a large margin, suggesting the assumed R value of 8 is likely to meet the FEMA defined standards to be considered the system R factor.

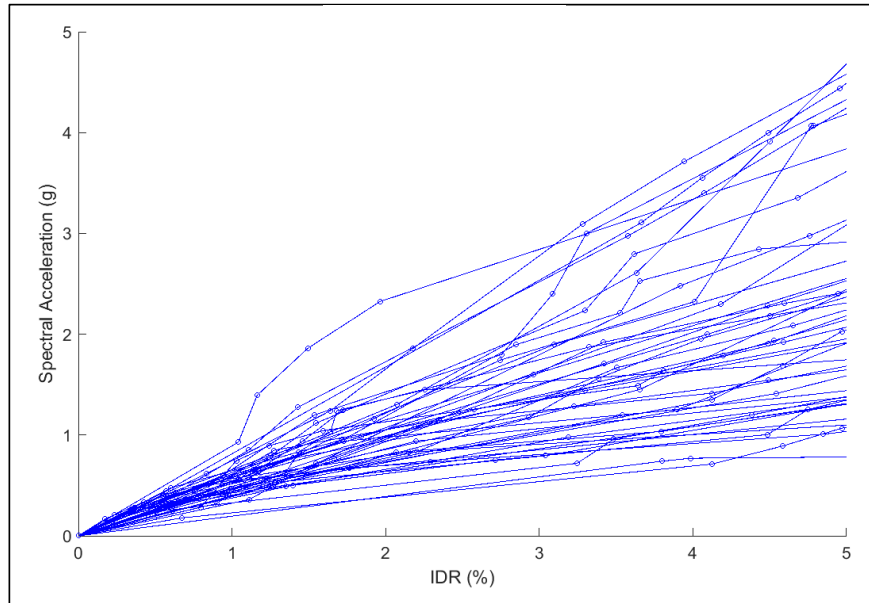


Figure 14: Spectral acceleration versus interstory drift ratio (IDR) for 44 FEMA P694 acceleration records

## 5. Conclusions

FEMA P695 analyses are currently underway for coupled composite plate shear walls - concrete-filled. Archetype structures have been designed to meet relevant code standards as well as enforce a strong wall-weak coupling beam approach. Experimental results from a companion research project, and those available in the literature, were used to develop and calibrate fiber-based models for the composite walls and concentrated plasticity-based models for the coupling beams. Preliminary results show that the system meets requirements for an R factor of 8 to be adopted, but further studies on the remainder of the archetype structures will need to be completed prior to affirming this conclusion.

## Acknowledgments

The project was supported by Charles Pankow Foundation (CPF Research Grant #06-16 and #05-17) and American Institute of Steel Construction (AISC). The authors would like to acknowledge these sponsors for their financial support and the members of the Peer-Review Panel Committee and Project Advisory Team for their technical guidance. The authors also acknowledge the contributions and support of Ron Klemencic and Brian Morgen from MKA Inc., and Michel Bruneau and Emre Kizilarslan from the Univ. at Buffalo. However, any opinions, findings, conclusions, and recommendations presented in this paper are those of the authors and do not necessarily reflect the view of the sponsors.

## References

- ACI Committee 318 (2014) *Building Code Requirements for Structural Concrete (ACI 318-14)*. American Concrete Institute.
- ASCE (2016). *Minimum design loads for buildings and other structures*, American Society of Civil Engineers.
- FEMA (2009). "FEMA P695: Quantification of Building Seismic Performance Factors." *Applied Technology Council. Federal Emergency Management Agency*.
- Lai, Z., Varma, A.H., and Zhang, K. (2014). "Noncompact or Slender Rectangular CFT Members: Experimental Database, Analysis and Design." *Journal of Constructional Steel Research*, 101(Oct), pp 455-468. <https://doi.org/10.1016/j.jcsr.2014.06.004>
- Lignos, D.G., and Krawinkler, H. (2011). "Deterioration modeling of steel components in support of collapse prediction of steel moment frames under earthquake loading", *Journal of Structural Engineering*, ASCE, 137 (11), 1291-1302.
- McKenna, F., Mazzoni, S., and Fenves, G. (2016). "Open System for Earthquake Engineering Simulation (OpenSees) Software Version 2.5.0" *University of California, Berkeley, CA. Available from <http://opensees.berkeley.edu>*.
- Nie, J.-G., Hu, H.-S., and Eatherton, M. R. (2014). "Concrete filled steel plate composite coupling beams: Experimental study." *Journal of Constructional Steel Research*, Elsevier, 94 49-63.
- Shafaei, S., Varma, A. H., Broberg, M., and Seo, J. (2019). "An Introduction to Numerical Modeling of Composite Plate Shear Walls / Concrete Filled (CPSW/CF)" *Proceedings of the Annual Stability Conference*, St. Louis, Missouri.
- Tao, Z., Wang, Z.-B., and Yu, Q. (2013). "Finite element modeling of concrete-filled steel stub columns under axial compression." *Journal of Constructional Steel Research*, Elsevier, 89 121–131.
- Wang, A., Seo, J., Shafaei, S., Varma, A., and Klemencic, R. (2018) "On the seismic behavior of concrete-filled composite plate shear walls." *Proceedings of the Eleventh U.S. National Conference on Earthquake Engineering*, Los Angeles, CA.